

Large deviations in non-Markovian stochastic epidemics

Matan Shmunik^a and Michael Assaf^a

^a*Racah Institute of Physics, The Hebrew University of Jerusalem, Jerusalem 91904, Israel*

We develop a framework for non-Markovian SIR and SIS models beyond mean field, utilizing the continuous-time random walk formalism. Using a gamma distribution for the infection and recovery inter-event times as a test case, we derive asymptotical late-time master equations with effective memory kernels and obtain analytical predictions for the final outbreak size distribution in the SIR model, and quasistationary distribution and disease lifetime in the SIS model. We show that increasing memory can greatly widen the outbreak size distribution and reduce the disease lifetime. We also show that rescaled Markovian models fail to capture fluctuations in the non-Markovian case. Overall, our findings, confirmed against numerical simulations, demonstrate that memory strongly shapes epidemic dynamics and paves the way for extending such analyses to structured populations.

Introduction. The challenge of modeling and predicting pandemics has motivated extensive development of deterministic and stochastic epidemiological models [1–8]. Their importance was underscored during COVID-19 [9, 10], when forecasts guided policies worldwide. These models typically divide populations into disease-status compartments. The SIS model [11] with susceptible and infected compartments, describes infections with short-lived immunity (e.g., influenza, or the common cold), while the SIR model [8] adds a recovered compartment to capture long-term immunity, which is relevant for diseases such as measles, smallpox, polio and COVID-19. Generalized models include reinfection (SIRS), an exposed compartment (SEIR) [6], time-varying rates [12, 13], or structured populations, where network-based approaches [14–19] capture heterogeneity in population structure. Mean-field quantities have been computed for both models: the mean outbreak size and epidemic threshold in the SIR model, and endemic state and relaxation dynamics in the SIS model [3, 5, 11, 14]. Stochastic dynamics have also been explored, including the outbreak-size distribution for the SIR model and quasistationary distribution (QSD) and disease mean time to extinction (MTE) for the SIS model [13, 20–30].

A key limitation of most approaches is the Markovian assumption [7, 31, 32]. In reality, infectious periods are often non-exponential, better described by log-normal, gamma, or Weibull distributions [33–35]. In structured populations the interactions may be diffusion-limited rather than reaction-limited, and cause heterogeneous, non-Markovian, infection times. Thus, infection and recovery are more realistically non-Markovian, but analytical methods developed for Markovian systems are generally ill-suited to handle such processes.

In the realm of epidemics, many studies have addressed non-Markovian processes [32, 36–48], mostly focusing on mean-field dynamics [39] and network generalizations [32, 38, 42–46]. In addition, Starnini *et al.* [48] showed that such dynamics can be reproduced by rescaling Markovian rates [49]. On the simulation side, Boguñá *et al.* [41] proposed a generalized Gillespie algorithm, later refined into the more efficient and accurate Laplace

Gillespie method by Masuda *et al.* [47]. Stochastic non-Markovian epidemics have also been studied in both SIR [36, 37, 40, 46] and SIS [38] models, but a systematic analysis of how non-Markovianity and demographic noise jointly shape large deviations is still lacking.

Recent progress has extended non-Markovian frameworks to chemical and biological systems. Aquino & Dentz [50] developed a formalism based on continuous-time random walk (CTRW) with non-exponential waiting times (WTs), later adapted in [51–53] to models of gene expression, population dynamics, and competition.

Here, we combine the WKB [22, 25, 54] approach of Hindes *et al.* [27] with the non-Markovian framework of Aquino *et al.* [50, 52] to study non-Markovian epidemic dynamics beyond mean field in a well-mixed setting. We compute the mean outbreak size and its full distribution within the SIR model, using gamma-distributed WTs as a prototypical example. We then analyze the SIS model, deriving the metastable mean, its full distribution, and MTE—the first passage time to the absorbing disease-free state [23, 55]. In both cases, we calculate memory kernels from general WT distributions and derive effective master equations using the final value theorem [50, 52]. Then, we apply the WKB approximation [25, 54] to obtain those key properties.

Non-Markovian SIR model. Within the well-mixed SIR model, given that the rates of infection and recovery per individual are β and γ , respectively, the discrete-state stochastic reactions can be written as $(S, I) \rightarrow (S-1, I+1)$ with mean rate $\beta SI/N$, and $(I, R) \rightarrow (I-1, R+1)$ with mean rate γI . Defining the population fractions as $x_s = S/N$, $x_i = I/N$ and $x_r = R/N$, assuming $N \gg 1$ and ignoring noise, the mean-field rate equations read

$$\dot{x}_s = -\beta x_s x_i, \quad \dot{x}_i = \beta x_s x_i - \gamma x_r, \quad \dot{x}_r = \gamma x_i, \quad (1)$$

such that $x_s + x_i + x_r = 1$. Here the underlying assumption is that reactions occur with exponential WTs. Yet, in reality, the WT distributions denoted by $\psi_1(t)$ for infection and $\psi_2(t)$ for recovery, are not necessarily exponential.

In this work we focus on an example of having Markovian infection and non-Markovian recovery, with a

gamma-distributed WT, while complementary cases and other WT choices are discussed in the Supplementary Information (SI) file. Here, the WT distributions satisfy

$$\psi_1(t) = \lambda_1 e^{-\lambda_1 t}, \quad \psi_2(t) = (\alpha \lambda_2)^\alpha t^{\alpha-1} e^{-\alpha \lambda_2 t} / \Gamma(\alpha), \quad (2)$$

where $\Gamma(a, z) = \int_z^\infty t^{a-1} e^{-t} dt$ is the incomplete gamma function. Notably, the WTs means are set to equal the Markovian counterparts, $\lambda_1 = N R_0 x_s x_i$ and $\lambda_2 = N x_i$ respectively, where $R_0 = \beta/\gamma$ is the basic reproductive number. The shape parameter α quantifies memory: small $\alpha \rightarrow 0$ yields a broad WT distribution, at $\alpha = 1$ it converges to the exponential distribution and as $\alpha \rightarrow \infty$ it approaches a deterministic (delta-like) process.

To determine the outbreak size distribution within the SIR model, we write the corresponding non-Markovian master equation for the probability $P_{S,I}$ to find S susceptibles and I infected at time t , which reads [51, 52]

$$\begin{aligned} \frac{\partial P_{S,I}}{\partial t} = & \int_0^t [M_1(S+1, I-1, t-t') P_{S+1, I-1}(t') \\ & - M_1(S, I, t-t') P_{S,I}(t') + M_2(S, I+1, t-t') P_{S, I+1}(t') \\ & - M_2(S, I, t-t') P_{S,I}(t')] dt'. \end{aligned} \quad (3)$$

In both infection and recovery, the dynamics depend on the full time history via the memory kernels M_i . The latter can be found by Laplace-transforming the master equation and using the specific structure of the WT distributions, $\psi_i(t)$, see SI, Sec. A. Even though the SIR dynamics has no metastability, and includes an infectious wave which quickly dies out, to explore the final outbreak distribution it suffices to look at the asymptotic late-time dependence of M_i in the limit of $t \rightarrow \infty$ [56]. Below we will also provide numerical justification for this claim. Thus, we use the final value theorem (FVT): $\lim_{t \rightarrow \infty} f(t) = \lim_{u \rightarrow 0} u \tilde{f}(u)$, for the memory kernel functions, where u is the Laplace variable. Defining the normalized asymptotic memory kernels: $\mathcal{M}_i := (1/N) \lim_{t \rightarrow \infty} M_i(t) = (1/N) \lim_{u \rightarrow 0} \tilde{M}_i(u)$ (see details in the SI, Sec. A) and using (3), we obtain the effective late-time master equation for the SIR model

$$\begin{aligned} \frac{\partial P_{S,I}}{\partial t} = & N [M_1(S+1, I-1) P_{S+1, I-1} - M_1(S, I) P_{S,I} \\ & + M_2(S, I+1) P_{S, I+1} - M_2(I) P_{S,I}], \end{aligned} \quad (4)$$

$$\text{with } \mathcal{M}_1 = R_0 x_i x_s, \quad \mathcal{M}_2 = \frac{R_0 x_i x_s}{(1 + R_0 x_s / \alpha)^\alpha - 1}. \quad (5)$$

This is one of the main results of this work. The asymptotic memory kernels, \mathcal{M}_1 and \mathcal{M}_2 are the effective infection and recovery rates under Markovian infection and non-Markovian (gamma-distributed) recovery. While for $\alpha = 1$ we recover the usual rate of x_i , decreasing α increases the recovery rate and greatly alters the dynamics.

Having found the effective rates, we now use the WKB approximation in the spirit of [27] to compute the final

outbreak size distribution; the WKB approximation is valid as long as $N \gg 1$ and the mean outbreak size is not too small. Substituting $P_{S,I} \sim e^{-N\mathcal{S}(x_s, x_i, t)}$ into Eq. (5) yields, in the leading order in $N \gg 1$, to a Hamilton-Jacobi equation $\partial \mathcal{S}(x_s, x_i, t) / \partial t + \mathcal{H}(x_s, x_i) = 0$, where $\mathcal{S}(x_s, x_i, t)$ is the action function, with the Hamiltonian

$$\mathcal{H} \equiv \mathcal{M}_1(x_s, x_i) (e^{p_i - p_s} - 1) + \mathcal{M}_2(x_s, x_i) (e^{-p_i} - 1). \quad (6)$$

Here, we have defined the momenta $p_i = \partial \mathcal{S} / \partial x_i$, $p_s = \partial \mathcal{S} / \partial x_s$ in analogy to classical mechanics. In the SI, Sec. B we show that p_i is a constant of motion, and use Hamilton's equations to derive a relation between p_i and final susceptible fraction $x_s^* = x_s(t \rightarrow \infty)$. Defining $m = e^{p_i}$, we find an implicit relation between m and x_s^*

$$\int_1^{x_s^*} [m (\mathcal{M}_1 / \mathcal{M}_2 + 1) - 1]^{-1} dx_s = \int_0^{1-x_s^*} dx_r. \quad (7)$$

This allows to compute the action function $\mathcal{S}(x_s, x_i, t) = \int_0^t (p_s \dot{x}_s + p_i \dot{x}_i - \mathcal{H}) dt'$ [27] (see SI, Sec. B), which reads

$$\mathcal{S}(x_s^*) = \int_1^{x_s^*} \ln \left\{ m^2 \mathcal{M}_1 / [m (\mathcal{M}_1 + \mathcal{M}_2) - \mathcal{M}_2] \right\} dx_s, \quad (8)$$

and is a function of x_s^* only via Eq. (7). Finally, the final outbreak distribution is $P(x_s^*) \sim e^{-N\mathcal{S}(x_s^*)}$.

To validate our theory, we run simulations using the next reaction method with simplified WT sampling [57], which in this case is accurate and faster compared to more elaborate Laplace- or non-Markovian-Gillespie schemes [41, 47]. In Fig. 1 we show examples of the final outbreak size distribution for four different α 's. Here, theory and simulations agree well as long as the final outbreak fraction $x_r^* = 1 - x_s^*$ is not too close to zero.

To quantify outbreak variability, we compute the standard deviation by expanding the action \mathcal{S} to second order around the mean final susceptible fraction \bar{x}_s^* , obtained at $p_s = p_i = 0$. Plugging this in Eq. (7) we get $\int_{\bar{x}_s^*}^1 (\mathcal{M}_2 / \mathcal{M}_1) dx_s = \int_0^{1-\bar{x}_s^*} dx_r$, an implicit equation for \bar{x}_s^* . Using \mathcal{M}_i from (5) yields: $\bar{x}_s^* = 1 - R_0^{-1} f(\bar{x}_s^*)$, with

$$f(\bar{x}_s^*) = B[(1 + \bar{x}_s^* R_0 / \alpha)^\alpha; 1/\alpha, 0] - B[(1 + R_0 / \alpha)^\alpha; 1/\alpha, 0],$$

where $B[x; a, b]$ is the incomplete beta function. Note that for $\alpha = 1$, the WT distribution becomes exponential, and we recover the known result of $1 - \bar{x}_s^* = -\ln \bar{x}_s^* / R_0$ [8].

Using the expression for the action \mathcal{S} , Eq. (8), we can derive the standard deviation σ by performing a Gaussian approximation on $P(x_s^*)$ around \bar{x}_s^* . This yields $\sigma \simeq | -N \mathcal{S}''(\bar{x}_s^*) |^{-1/2}$, which can be directly compared to simulation results. Figure 2 shows the effect of varying the shape parameter α for gamma-distributed recovery with exponential infection: as α decreases, the mean outbreak size drops (since typical recovery times are shorter than in the Markovian case) while the standard deviation increases. We also see that the WKB approximation

breaks down when the mean outbreak size nears zero.

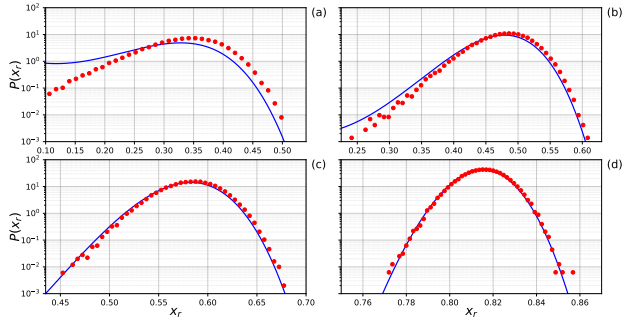


FIG. 1. Outbreak size distributions at $\alpha = 0.65, 0.8, 1$ and 10 in (a)–(d), for Markovian infection and gamma-distributed recovery, $N = 5000$, $R_0 = 1.5$, and 10^4 runs per α . Simulations (symbols) are compared with theory (solid line). In all panels $I(0) = 1$, and outbreak fractions $< 10^{-2}$ were omitted.

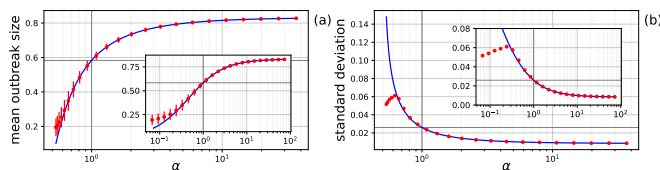


FIG. 2. Normalized mean x_r^* (a) and normalized standard deviation σ (b) versus α . Insets show those quantities versus $\tilde{\alpha} \equiv (\alpha - \alpha_{bif})/\alpha_{bif}$, where at α_{bif} the mean vanishes. Here infection is exponential and recovery is gamma-distributed, $N = 5000$, $R_0 = 1.5$, $\alpha_{bif} \simeq 0.5$, and 10^4 runs per α . Simulations (symbols) are compared with theory (solid line). In all panels $I(0) = 1$, and outbreak fractions $< 10^{-2}$ were omitted.

Non-Markovian SIS model. Here, a susceptible can get infected at a rate β and infected individuals recover at a rate γ . The Markovian mean-field dynamics satisfy $\dot{x}_i = \beta x_s x_i - \gamma x_i$, where $x_i + x_s = 1$. Notably, the late-time dynamics of this model are markedly different from the SIR model. Here, for $N \gg 1$, the system enters a long-lived metastable state, which then slowly decays due to an exponentially-small probability flux into the absorbing state at $I = 0$. As we are interested in finding the statistics of the metastable state and MTE, we again use the long-time effective memory kernels defined above, and arrive at the late-time master equation

$$\begin{aligned} \partial P_I / \partial t = & N [\mathcal{M}_1(I-1)P_{I-1} - \mathcal{M}_1(I)P_I \\ & + \mathcal{M}_2(I+1)P_{I+1} - \mathcal{M}_2(I)P_I]. \end{aligned} \quad (9)$$

This master equation is valid after the initial relaxation period near the endemic state, τ_r , which we compute below, and \mathcal{M}_i are given by Eq. (5) with $x_s = 1 - x_i$.

To quantify the effect of non-Markovian recovery on the endemic state x_i^* , we multiply Eq. (9) by I and sum over all I . This yields the modified rate equation $\langle \dot{x}_i \rangle = \mathcal{M}_1(\langle x_i \rangle) - \mathcal{M}_2(\langle x_i \rangle)$, with x_i^* found by solving $\mathcal{M}_1(x_i^*) = \mathcal{M}_2(x_i^*)$. Using (5) with $x_s = 1 - x_i$ gives

$$x_i^* = 1 - (\alpha/R_0)(2^{1/\alpha} - 1). \quad (10)$$

At $\alpha = 1$ (exponential WTs), we recover the Markovian result $x_i^* = 1 - 1/R_0$ with a bifurcation at $R_0 = 1$. For $\alpha \neq 1$, the bifurcation shifts to $R_{bif} = \alpha(2^{1/\alpha} - 1)$: it moves above 1 for $\alpha < 1$ and below 1 for $\alpha > 1$. Consequently, we find that an endemic state can persist even when each infected transmits to fewer than one other individual, or conversely, a highly infectious disease may still die out exponentially fast. Note that the relaxation time of the dynamics $\tau_r = [\mathcal{M}_2'(x_i^*) - \mathcal{M}_1'(x_i^*)]^{-1}$ can also be computed. Using Eq. (5) we obtain $\tau_r = 2^{1/\alpha-1} / \{\alpha(2^{1/\alpha} - 1)[R_0 - \alpha(2^{1/\alpha} - 1)]\}$, which coincides with the known result of $\tau_r = 1/(R_0 - 1)$ at $\alpha = 1$.

We now analyze the effective master equation (9) to determine the QSD of the metastable state and the MTE under non-Markovian recovery. Assuming the metastable state decays slowly, we set $P_I(t) = \pi(x_i)e^{-t/\tau_{ext}}$, where $\pi(x_i)$ is the QSD and τ_{ext} is the exponentially large MTE. We now apply the WKB approximation, $\pi(x_i) \sim e^{-N\mathcal{S}(x_i)}$, where $\mathcal{S}(x_i)$ is the action function. Expanding to leading order in $N \gg 1$, and using Eq. (5) we obtain $\mathcal{S}'(x_i) = -\ln[\mathcal{M}_1(x_i)/\mathcal{M}_2(x_i)] = -\ln[(1 + R_0(1 - x_i)/\alpha)^\alpha - 1]$, which provides the QSD $\pi(x_i)$

$$\pi(x_i) \sim e^{-N \int_{x_i^*}^{x_i} \ln[\mathcal{M}_2(x')/\mathcal{M}_1(x')] dx'}. \quad (11)$$

The QSD can be explicitly written using Eq. (5) in terms of the ${}_2F_1(a, b; c; z)$ hypergeometric function, and generalizes the result for Markovian reactions [20, 23]. In Fig. 3 we show excellent agreement between simulated QSDs for various values of α and our theoretical prediction. We also plot by dashed lines the QSDs that would be obtained if we use a Markovian theory with adjusted reaction rates, obtained by replacing the gamma-distributed recovery process with an exponential one, and adjusting the infection rate by $R_0 \rightarrow R_0/R_{bif}$. While being a good approximation close to the mean, the tails are clearly missed by this adjusted distribution, which demonstrates that the non-Markovian effects cannot be fully captured by simply adjusting the mean of a Markovian reaction.

We can also compute the QSD's standard deviation σ by approximating $\pi(x_i)$ as a Gaussian around x_i^* [23], which yields $\sigma = |-NS''(x_i^*)|^{-1/2}$. Using Eq. (5) we find

$$\sigma = \sqrt{2^{1/\alpha-1}/(NR_0)} = \sqrt{(1-x_i^*)/[2\alpha N(1-2^{-1/\alpha})]}. \quad (12)$$

First of all, at $\alpha = 1$ we recover the Markovian result of $\sigma = (NR_0)^{-1/2}$. Second, as α decreases below 1, the standard deviation, or typical fluctuations, can greatly increase, making disease extinction much more likely, see below. In fact, we can approximate α close to 1 to obtain $\sigma = (NR_0)^{-1/2} [1 + \ln 2/2(1 - \alpha)]$, from which it is clear that as α decreases below 1, the variance grows.

In Fig. 4(a,b) we show how the shape parameter α affects the metastable mean (10) and its standard deviation (12), both normalized by their Markovian values

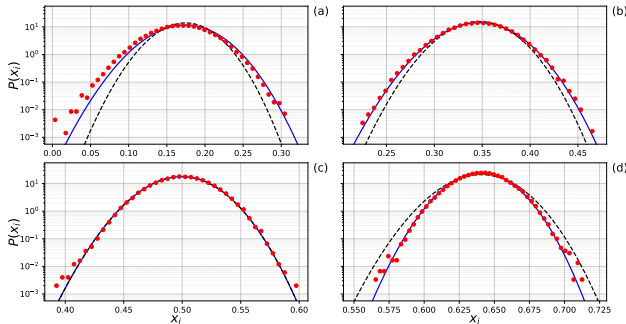


FIG. 3. QSDs at $\alpha = 0.45, 0.6, 1, 10$ in (a)–(d), for Markovian infection and gamma-distributed recovery, with $N = 1000$, $R_0 = 2$ and 10^5 runs per α . Here we compare simulations (symbols) to theory (solid line) and to a Markovian theory adjusted to the same mean (dashed line), with $x_i(0) = x_i^*$.

($x_i^*(1) = 1/3$, $\sigma(1) \approx 0.0258$ for $R_0 = 1.5$). As α decreases, the mean drastically decreases and the variance increases; this is since the typical time between recovery events gets shorter as the WT distribution becomes wider and more skewed. The opposite occurs for $\alpha > 1$; for $\alpha \rightarrow \infty$, the mean approaches $x_i^*(\infty)/x_i^*(1) \simeq (1 - \ln 2/R_0)/(1/3) \simeq 1.614$. Near the bifurcation, the mean vanishes and the WKB approximation breaks down.

The dependence of the variance on α as observed in Fig. 4(b) can be explained by looking at the right-hand-side of Eq. (12), where the standard deviation is expressed as a function of the mean x_i^* and α , assuming the effect of non-Markovianity on the mean is corrected by adjusting R_0 [58]. This reveals three effects shaping σ . The first and strongest is the monotone relation $\sigma \sim \sqrt{1 - x_i^*}$, dominating the behavior. The second stems from non-Markovianity, $\sigma \sim [2\alpha(1 - 2^{-1/\alpha})]^{-1/2}$; it reinforces the main effect in the non-Markovian recovery case of increase of σ as α is decreased (but partially opposes it for non-Markovian infection, see SI, Sec. C). The third arises from WKB breakdown: as x_i^* approaches 0, the monotone relation fails, and σ begins to decrease with x_i^* , as fluctuations near 0 are constrained by the boundary (similarly as when x_i^* approaches 1).

Finally, having computed the complete QSD (11), we can evaluate the MTE, using $\tau_{ext} \sim e^{NS(0)}$ [23, 25, 54], which gives rise to an explicit expression containing the hypergeometric function ${}_2F_1(a, b; c; z)$. A simplified expression can be obtained, in the limit of $|\alpha - 1| \ll 1$, which can provide insight on how the disease lifetime changes as one slightly deviates from Markovianity. Approximating $S(0)$ in the leading order in $|\alpha - 1| \ll 1$, we find

$$S(0) \simeq \ln R_0 + R_0^{-1} - 1 - \{\ln(R_0 + 1) - 2 - R_0^{-1}[\pi^2/12 - 2 + 2 \ln 2 - \ln(R_0 + 1) + \text{Li}_2(-R_0)]\}(1 - \alpha), \quad (13)$$

where $\text{Li}_2(z)$ is the second polylogarithm. Note that we recover the known result of $S(0) = 1 - \ln R_0 - 1/R_0$ at $\alpha = 1$ [20, 22, 23, 25]. In Fig. 4(c) we plot the MTE

versus α for exponential infection and gamma-distributed recovery. Good agreement holds as long as the action is large (i.e., $\ln \tau_{ext} \gg 1$). We also show the approximate theoretical result close to $\alpha = 1$, which excellently agrees with simulations well beyond its region of applicability.

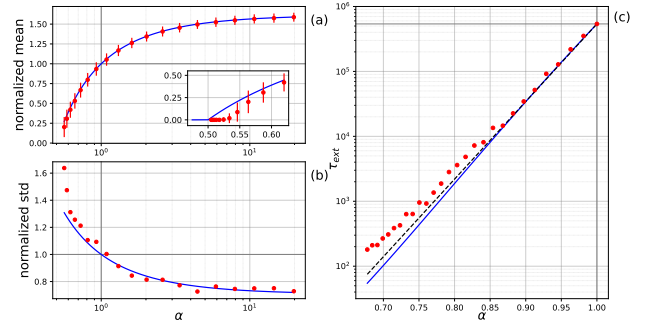


FIG. 4. Normalized mean x_i^* (a) and normalized standard deviation σ (b) vs α , for Markovian infection and gamma-distributed recovery, $N = 1000$, $R_0 = 1.5$, and 10^3 runs per α . Inset zooms in close to the bifurcation. Simulations (symbols) are compared with theory (solid line). In (c) we plot the MTE vs α for the same WTs, $N = 180$, $R_0 = 1.5$, and 10^2 runs per α . Simulations (symbols) are compared with theory (solid line) and Eq. (13) (dashed line). In all panels $x_i(0) = x_i^*$.

Conclusion. We studied how non-Markovian infection and recovery WTs shape long-term epidemic dynamics. For both the SIR and SIS models, we derived an effective asymptotic master equation, valid at late times, by explicitly computing the memory kernels given the WT distributions. Within the SIR model we showed that non-Markovian recovery can drastically increase the final outbreak size distribution’s width, which may have key implications on pandemics handling. Within the SIS model, we computed the QSD of the long-lived metastable state and the MTE, and showed that the latter can greatly decrease as memory strength increases, making epidemics far more fragile to extinction. Finally, we checked that other WT distributions (e.g., power laws) give rise to qualitatively similar behavior, see SI, Sec. D.

In future work, it is desirable to compare our predictions to realistic non-Markovian epidemic scenarios with empirical WT distributions. In addition, while mean-field impacts of non-Markovian epidemics on *structured populations* were recently analyzed, stochastic fluctuations remain largely unexplored. Capturing them will likely require a modified formalism to handle non-resetting reactions that are able to account for memory effects in heterogeneous contact structures.

- [1] R. M. Anderson and R. M. May, *Infectious diseases of humans: dynamics and control* (Oxford university press, 1991).
- [2] W. O. Kermack and A. G. McKendrick, A contribution to the mathematical theory of epidemics, Proceedings of

- the royal society of london. Series A, Containing papers of a mathematical and physical character **115**, 700 (1927).
- [3] L. J. Allen, Some discrete-time si, sir, and sis epidemic models, *Mathematical biosciences* **124**, 83 (1994).
 - [4] D. Mollison, *Epidemic models: their structure and relation to data*, 5 (Cambridge University Press, 1995).
 - [5] D. J. Daley and J. M. Gani, *Epidemic modelling: an introduction*, 15 (Cambridge University Press, 1999).
 - [6] H. W. Hethcote, The mathematics of infectious diseases, *SIAM review* **42**, 599 (2000).
 - [7] M. J. Keeling and K. T. Eames, Networks and epidemic models, *Journal of the royal society interface* **2**, 295 (2005).
 - [8] J. Neipel, J. Bauermann, S. Bo, T. Harmon, and F. Jülicher, Power-law population heterogeneity governs epidemic waves, *PloS one* **15**, e0239678 (2020).
 - [9] W. Yang, D. Zhang, L. Peng, C. Zhuge, and L. Hong, Rational evaluation of various epidemic models based on the covid-19 data of china, *Epidemics* **37**, 100501 (2021).
 - [10] Modeling covid-19 scenarios for the united states, *Nature medicine* **27**, 94 (2021).
 - [11] H. W. Hethcote, Three basic epidemiological models, in *Applied mathematical ecology* (Springer, 1989) pp. 119–144.
 - [12] J. L. Aron and I. B. Schwartz, Seasonality and period-doubling bifurcations in an epidemic model, *Journal of theoretical biology* **110**, 665 (1984).
 - [13] L. B. Shaw and I. B. Schwartz, Fluctuating epidemics on adaptive networks, *Physical Review E—Statistical, Nonlinear, and Soft Matter Physics* **77**, 066101 (2008).
 - [14] R. Pastor-Satorras, C. Castellano, P. Van Mieghem, and A. Vespignani, Epidemic processes in complex networks, *Reviews of modern physics* **87**, 925 (2015).
 - [15] B. Karrer and M. E. Newman, Message passing approach for general epidemic models, *Physical Review E—Statistical, Nonlinear, and Soft Matter Physics* **82**, 016101 (2010).
 - [16] J. Lindquist, J. Ma, P. van den Driessche, and F. H. Willeboordse, Effective degree network disease models, *Journal of mathematical biology* **62**, 143 (2011).
 - [17] J. C. Miller, A. C. Slim, and E. M. Volz, Edge-based compartmental modelling for infectious disease spread, *Journal of the Royal Society Interface* **9**, 890 (2012).
 - [18] M. J. Keeling, The effects of local spatial structure on epidemiological invasions, *Proceedings of the Royal Society of London. Series B: Biological Sciences* **266**, 859 (1999).
 - [19] T. House and M. J. Keeling, Insights from unifying modern approximations to infections on networks, *Journal of The Royal Society Interface* **8**, 67 (2011).
 - [20] O. Ovaskainen, The quasistationary distribution of the stochastic logistic model, *Journal of Applied Probability* **38**, 898 (2001).
 - [21] M. I. Dykman, I. B. Schwartz, and A. S. Landsman, Disease extinction in the presence of random vaccination, *Physical review letters* **101**, 078101 (2008).
 - [22] O. Ovaskainen and B. Meerson, Stochastic models of population extinction, *Trends in ecology & evolution* **25**, 643 (2010).
 - [23] M. Assaf and B. Meerson, Extinction of metastable stochastic populations, *Physical Review E—Statistical, Nonlinear, and Soft Matter Physics* **81**, 021116 (2010).
 - [24] J. Hindes and I. B. Schwartz, Epidemic extinction and control in heterogeneous networks, *Physical review letters* **117**, 028302 (2016).
 - [25] M. Assaf and B. Meerson, Wkb theory of large deviations in stochastic populations, *Journal of Physics A: Mathematical and Theoretical* **50**, 263001 (2017).
 - [26] J. Hindes and M. Assaf, Degree dispersion increases the rate of rare events in population networks, *Physical review letters* **123**, 068301 (2019).
 - [27] J. Hindes, M. Assaf, and I. B. Schwartz, Outbreak size distribution in stochastic epidemic models, *Physical Review Letters* **128**, 078301 (2022).
 - [28] J. Hindes, L. Mier-y Teran-Romero, I. B. Schwartz, and M. Assaf, Outbreak-size distributions under fluctuating rates, *Physical Review Research* **5**, 043264 (2023).
 - [29] E. Korngut, O. Vilks, and M. Assaf, Weighted-ensemble network simulations of the susceptible-infected-susceptible model of epidemics, *Physical Review E* **111**, 014146 (2025).
 - [30] E. Korngut and M. Assaf, Impact of network assortativity on disease lifetime in the sis model of epidemics, *Physical Review E* **112**, 024302 (2025).
 - [31] E. Volz, Sir dynamics in random networks with heterogeneous connectivity, *Journal of mathematical biology* **56**, 293 (2008).
 - [32] N. Sherborne, J. C. Miller, K. B. Blyuss, and I. Z. Kiss, Mean-field models for non-markovian epidemics on networks, *Journal of mathematical biology* **76**, 755 (2018).
 - [33] N. T. Bailey, A statistical method of estimating the periods of incubation and infection of an infectious disease, *Nature* **174**, 139 (1954).
 - [34] K. Gough, The estimation of latent and infectious periods, *Biometrika* **64**, 559 (1977).
 - [35] H. J. Wearing, P. Rohani, and M. J. Keeling, Appropriate models for the management of infectious diseases, *PLoS medicine* **2**, e174 (2005).
 - [36] F. Ball, A unified approach to the distribution of total size and total area under the trajectory of infectives in epidemic models, *Advances in Applied Probability* **18**, 289 (1986).
 - [37] A. Startsev, On the distribution of the size of an epidemic in a non-markovian model, *Theory of Probability & Its Applications* **41**, 730 (1997).
 - [38] E. Cator, R. Van de Bovenkamp, and P. Van Mieghem, Susceptible-infected-susceptible epidemics on networks with general infection and cure times, *Physical Review E—Statistical, Nonlinear, and Soft Matter Physics* **87**, 062816 (2013).
 - [39] P. Van Mieghem and R. Van de Bovenkamp, Non-markovian infection spread dramatically alters the susceptible-infected-susceptible epidemic threshold in networks, *Physical review letters* **110**, 108701 (2013).
 - [40] D. Clancy, Sir epidemic models with general infectious period distribution, *Statistics & Probability Letters* **85**, 1 (2014).
 - [41] M. Boguná, L. F. Lafuerza, R. Toral, and M. Á. Serrano, Simulating non-markovian stochastic processes, *Physical Review E* **90**, 042108 (2014).
 - [42] I. Z. Kiss, G. Röst, and Z. Vizi, Generalization of pairwise models to non-markovian epidemics on networks, *Physical review letters* **115**, 078701 (2015).
 - [43] G. Röst, Z. Vizi, and I. Z. Kiss, Impact of non-markovian recovery on network epidemics, *Biomat* , 40 (2015).
 - [44] I. Z. Kiss, J. C. Miller, and P. L. Simon, Non-markovian epidemics, in *Mathematics of Epidemics on Networks:*

From Exact to Approximate Models (Springer International Publishing, Cham, 2017) pp. 303–326.

- [45] G. Röst, Z. Vizi, and I. Kiss, Pairwise approximation for sir-type network epidemics with non-markovian recovery, *Proceedings of the Royal Society A: Mathematical, Physical and Engineering Sciences* **474**, 20170695 (2018).
- [46] R. R. Wilkinson and K. J. Sharkey, Impact of the infectious period on epidemics, *Physical Review E* **97**, 052403 (2018).
- [47] N. Masuda and L. E. Rocha, A gillespie algorithm for non-markovian stochastic processes, *Siam Review* **60**, 95 (2018).
- [48] M. Starnini, J. P. Gleeson, and M. Boguñá, Equivalence between non-markovian and markovian dynamics in epidemic spreading processes, *Physical review letters* **118**, 128301 (2017).
- [49] M. Feng, S.-M. Cai, M. Tang, and Y.-C. Lai, Equivalence and its invalidation between non-markovian and markovian spreading dynamics on complex networks, *Nature communications* **10**, 3748 (2019).
- [50] T. Aquino and M. Dentz, Chemical continuous time random walks, *Physical review letters* **119**, 230601 (2017).
- [51] O. Vilks, R. Metzler, and M. Assaf, Non-markovian gene expression, *Physical Review Research* **6**, L022026 (2024).
- [52] O. Vilks and M. Assaf, Escape from a metastable state in non-markovian population dynamics, *Physical Review E* **110**, 044132 (2024).
- [53] O. Vilks, M. Mobilia, and M. Assaf, Non-markovian rock-paper-scissors games, *Physical Review Research* **7**, 023284 (2025).
- [54] M. I. Dykman, E. Mori, J. Ross, and P. Hunt, Large fluctuations and optimal paths in chemical kinetics, *The Journal of chemical physics* **100**, 5735 (1994).
- [55] S. Redner, *A guide to first-passage processes* (Cambridge university press, 2001).
- [56] This is justified by the fact that for $N \gg 1$ the epidemic duration is still much longer than the typical relaxation time of the system [59].
- [57] D. F. Anderson, A modified next reaction method for simulating chemical systems with time dependent propensities and delays, *The Journal of chemical physics* **127** (2007).
- [58] Notably, the dependence of σ on x_i^* and α remains identical also when infection is gamma-distributed and recovery is exponential, even though x_i^* changes in that case.
- [59] M. Turkyilmazoglu, Explicit formulae for the peak time of an epidemic from the sir model, *Physica D: Nonlinear Phenomena* **422**, 132902 (2021).

Supplemental Information

A. OBTAINING THE NON-MARKOVIAN MASTER EQUATION

We begin by showing how the non-Markovian infection and recovery processes can be formulated. In this aspect, the analysis of the SIS and SIR models will be identical, but later the treatment of the master equation will be different depending on the model at hand. We start by computing the survival probabilities corresponding to the WT distributions defined in the main text

$$\Psi_1(t) = e^{-\lambda_1 t}, \quad \Psi_2(t) = \frac{\Gamma(\alpha, \alpha \lambda_2 t)}{\Gamma(\alpha)}. \quad (\text{S1})$$

We next calculate $\phi_1(t)$ —the distribution for a single infection event to occur at time t , assuming no recovery has occurred up to t , and $\phi_2(t)$ —the distribution for a single recovery event to occur at time t , assuming no infection has occurred up to t . This yields $\phi_1(t) = \psi_1(t)\Psi_2(t)$, $\phi_2(t) = \psi_2(t)\Psi_1(t)$, and with Eq. (2) in the main text we get

$$\begin{aligned} \phi_1(t) &= NR_0 x_s x_i \frac{\Gamma(\alpha, \alpha N x_i t)}{\Gamma(\alpha)} e^{-NR_0 x_s x_i t}, \\ \phi_2(t) &= \frac{(\alpha N x_i)^{a-1} e^{-\alpha N x_i t}}{\Gamma(a)} e^{-NR_0 x_s x_i t}. \end{aligned} \quad (\text{S2})$$

where $\Gamma(a, z) = \int_z^\infty t^{a-1} e^{-t} dt$ is the incomplete gamma function. We then calculate the Laplace transform of $\tilde{\phi}_i$:

$$\begin{aligned} \tilde{\phi}_1(u) &= \frac{NR_0 x_s x_i}{u + NR_0 x_s x_i} \left[1 - \left(1 + \frac{u}{\alpha N x_i} + \frac{R_0 x_s}{\alpha} \right)^{-\alpha} \right], \\ \tilde{\phi}_2(u) &= \left(1 + \frac{u}{\alpha N x_i} + \frac{R_0 x_s}{\alpha} \right)^{-\alpha}, \end{aligned} \quad (\text{S3})$$

where u is the Laplace variable. Using these quantities, and the framework developed in [51, 52], we can compute $\tilde{M}_i(u)$ —the Laplace transform of the memory kernels $M_i(t)$, which enter the non-Markovian master equation [Eq. (3) in the main text]—multiplied by the Laplace parameter u . This yields

$$\tilde{M}_i(u) := u\mathcal{L}[M_i(t)] = \frac{u\tilde{\phi}_i(u)}{1 - \tilde{\phi}_1(u) - \tilde{\phi}_2(u)}. \quad (\text{S4})$$

As stated, the inverse Laplace transform of these memory kernels in Laplace space will enter the non-Markovian master equation, see Eq. (3) in the main text. Performing the explicit calculation of these memory kernels using

Eq. (S4), we find

$$\begin{aligned} \tilde{M}_1(u) &= NR_0 x_i x_s, \\ \tilde{M}_2(u) &= \frac{u + NR_0 x_i x_s}{[1 + u/(\alpha N x_i) + R_0 x_s/\alpha]^\alpha - 1}. \end{aligned} \quad (\text{S5})$$

Finally, we use the finite value theorem $\lim_{t \rightarrow \infty} f(t) = \lim_{u \rightarrow 0} u\tilde{f}(u)$, and define the normalized asymptotic memory kernel \mathcal{M}_i as: $\mathcal{M}_i := (1/N) \lim_{t \rightarrow \infty} M_i(t) = (1/N) \lim_{u \rightarrow 0} \tilde{M}_i(u)$ to get Eq. (4) and Eq. (5) in the main text.

B. DERIVATION OF THE FINAL OUTBREAK-SIZE DISTRIBUTION

To compute the final outbreak size distribution in the realm of the SIR model, we employ the Hamiltonian formalism. Starting from the Hamiltonian

$$\mathcal{H} \equiv \mathcal{M}_1(x_s, x_i) (e^{p_i - p_s} - 1) + \mathcal{M}_2(x_s, x_i) (e^{-p_i} - 1), \quad (\text{S6})$$

we write down Hamilton's equations

$$\dot{x}_s = \frac{\partial \mathcal{H}}{\partial p_s} = -\mathcal{M}_1 e^{p_i - p_s}, \quad (\text{S7})$$

$$\dot{x}_i = \frac{\partial \mathcal{H}}{\partial p_i} = \mathcal{M}_1 e^{p_i - p_s} - \mathcal{M}_2 e^{-p_i}, \quad (\text{S8})$$

$$\dot{p}_s = -\frac{\partial \mathcal{H}}{\partial x_s} = \frac{\partial \mathcal{M}_1}{\partial x_s} (1 - e^{p_i - p_s}) + \frac{\partial \mathcal{M}_2}{\partial x_s} (1 - e^{-p_i}), \quad (\text{S9})$$

$$\dot{p}_i = -\frac{\partial \mathcal{H}}{\partial x_i} = \frac{\partial \mathcal{M}_1}{\partial x_i} (1 - e^{p_i - p_s}) + \frac{\partial \mathcal{M}_2}{\partial x_i} (1 - e^{-p_i}). \quad (\text{S10})$$

The solutions of these equations yield, among other insights, the most probable outbreak dynamics and enables the determination of both the mean outbreak size as well as the full outbreak-size distribution.

Before delving into these equations we point out an important constant of motion, which appears in the SIR model and enables the intrinsically two-dimensional problem to be cast into one dimension. First, we point out that the Hamiltonian is a constant of motion, since the rates do not depend on time explicitly. Furthermore, when examining the rates \mathcal{M}_i we can see that in our example case they are both linear in x_i , see Eq. (5) in the main text. This attribute also holds for a wide variety of other WT distributions such as a power-law distribution, see SI Sec. D. As a result, using Eqs. (S6) and (S10), we can write the Hamiltonian in a suggestive way $\mathcal{H} = -x_i \dot{p}_i$. Finally, since most epidemic waves start from a small fraction of infected, we argue that typically $x_i(t=0) \ll 1$, and is certainly not macroscopic; in fact, it is often assumed that one starts with one infected individual such that $x_i(t=0) \sim O(1/N)$ with $N \gg 1$. As a result, since $\mathcal{H}(t=0)$ is a constant of motion, one must have $\mathcal{H} \simeq 0$ throughout the epidemic. Yet, due to the

fact that $\mathcal{H} = -x_i \dot{p}_i$, and that $x_i(t)$ changes from a very small value to a macroscopic fraction of the population during the epidemic wave, the only way the Hamiltonian can stay zero is by having $\dot{p}_i = 0$ throughout it. Therefore, we have found a new constant of motion: p_i .

Notably, even though in this case $\mathcal{H} \simeq 0$, there is an important distinction between our use of the WKB assumption here and in the SIS model. While the condition of $\mathcal{H} \simeq 0$ is inherent in the SIS model as the distribution becomes metastable with $\partial P(x_i, t)/\partial t \simeq 0$ (up to exponential accuracy), in the SIR model this condition solely stems from starting with a small fraction of infected individuals.

We now derive the outbreak size distribution by adopting the methodology of [27] and defining a new constant of motion $m = e^{p_i}$. Using Eqs. (S7) and (S8) and the fact that the total population is constant, i.e. $\dot{x}_s + \dot{x}_i + \dot{x}_r = 0$, we get an equation for \dot{x}_r

$$\dot{x}_r = -\dot{x}_s - \dot{x}_i = \mathcal{M}_2/m. \quad (\text{S11})$$

By equating the Hamiltonian [Eq. (S6)] to zero, we can get an expression for e^{p_s}

$$e^{p_s} = \frac{m^2 \mathcal{M}_1 / \mathcal{M}_2}{m(\mathcal{M}_1 / \mathcal{M}_2 + 1) - 1}. \quad (\text{S12})$$

Now we divide Eq. (S7) by (S11) to obtain a differential equation for the dependence of x_s on x_r

$$\frac{dx_s}{dx_r} = -\frac{\mathcal{M}_1}{\mathcal{M}_2} m^2 e^{-p_s} = 1 - m \left(\frac{\mathcal{M}_1}{\mathcal{M}_2} + 1 \right). \quad (\text{S13})$$

By integrating x_s from 1 to x_s^* and x_r from 0 to $1 - x_s^*$, we obtain an implicit relation between the final outbreak size $x_s^* = x_s(t \rightarrow \infty)$ and m

$$\int_1^{x_s^*} \frac{1}{m(\mathcal{M}_1 / \mathcal{M}_2 + 1) - 1} dx_s = \int_0^{1-x_s^*} dx_r. \quad (\text{S14})$$

Note that, plugging $\alpha = 1$ into \mathcal{M}_1 and \mathcal{M}_2 and using Eq. (5) in the main text, this result coincides with that of Ref. [27] in the Markovian case. Equation (S14) is important since it removes m from the action \mathcal{S} and makes it a function of a single variable x_s^* . To find the action $\mathcal{S}(x_s^*)$ for each final state x_s^* , which determines the outbreak size distribution via the WKB ansatz, we write down the formal solution of the action, as done in classical mechanics [23,25,27]

$$\mathcal{S}(x_s, x_i, t) = \int_0^t (p_s \dot{x}_s + p_i \dot{x}_i - \mathcal{H}) dt'. \quad (\text{S15})$$

We argue that the integral over \mathcal{H} vanishes because $\mathcal{H} \simeq 0$, and that when taking $t \rightarrow \infty$ the integral over $p_i \dot{x}_i$ vanishes because p_i is constant and $x_i(t=0) = x_i(t \rightarrow \infty) \simeq 0$. After some algebra, this leaves us with

a reduced integral $\mathcal{S}(x_s^*) = \int_1^{x_s^*} p_s dx_s$, where p_s is given by Eq. (S12). Plugging p_s into the integral, we obtain

$$\mathcal{S}(x_s^*) = \int_1^{x_s^*} \ln \left\{ m^2 \mathcal{M}_1 / [m(\mathcal{M}_1 + \mathcal{M}_2) - \mathcal{M}_2] \right\} dx_s, \quad (\text{S16})$$

which coincides with Eq. (8) in the main text. This allows finding the final outbreak-size distribution in the presence of non-Markovian reactions.

C. SIS MODEL UNDER NON-MARKOVIAN INFECTION

C1. Non-Markovian infection and Markovian recovery

In this section we consider the complementary case of non-Markovian infection with Markovian or non-Markovian recovery. Let us start with Markovian (exponential) recovery and gamma-distributed infection. Here, the WTs satisfy

$$\psi_1(t) = \frac{(\alpha \lambda_1)^{\alpha} t^{\alpha-1} e^{-\alpha \lambda_1 t}}{\Gamma(\alpha)}, \quad \psi_2(t) = \lambda_2 e^{-\lambda_2 t}, \quad (\text{S17})$$

with means of $\lambda_1 = NR_0 x_s x_i$ and $\lambda_2 = N x_i$.

We can now repeat the calculations done in the main text for this case and compute the quasistationary (QSD) distribution in the long-lived metastable state within the SIS model. In Fig. S1 we show how varying the shape parameter α affects the QSD's mean and its standard deviation for gamma-distributed infection and exponential recovery. Normalization of the mean and standard deviation is performed as in Fig. 4 in the main text. Unlike the recovery case in Fig. 4, here increasing α leads to a larger standard deviation and a smaller mean. The disagreement with the theory here again occurs as the mean decreases towards 0 and the WKB theory becomes invalid.

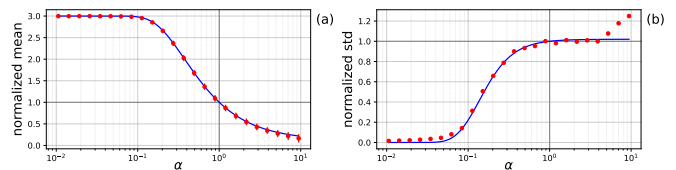


FIG. S1. The normalized mean x_i^* (a) and normalized standard deviation σ (b) as functions of α , for gamma-distributed infection and exponentially-distributed recovery, $N = 1000$, $R_0 = 1.5$, and 10^3 runs per α . Simulations (symbols) are compared with theory (blue solid line). In all panels the initial conditions was $x_i(0) = x_i^*$.

C2. Non-Markovian infection and recovery

One can also consider the case of non-Markovian infection and recovery, with WTs both distributed according to the gamma distribution. In this case the WTs satisfy

$$\psi_1(t) = \frac{(\alpha\lambda_1)^\alpha t^{\alpha-1} e^{-\alpha\lambda_1 t}}{\Gamma(\alpha)}, \quad \psi_2(t) = \frac{(\alpha\lambda_2)^\alpha t^{\alpha-1} e^{-\alpha\lambda_2 t}}{\Gamma(\alpha)}, \quad (\text{S18})$$

with means of $\lambda_1 = NR_0 x_s x_i$ and $\lambda_2 = Nx_i$.

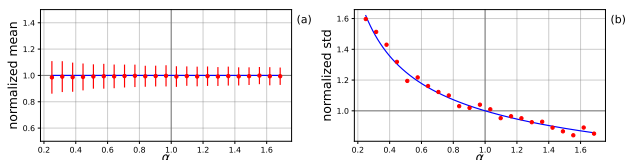


FIG. S2. The normalized mean x_i^* (a) and normalized standard deviation σ (b) as functions of α , for gamma-distributed infection and gamma-distributed recovery, $N = 5000$, $R_0 = 1.5$, and 10^4 runs per α . Simulations (symbols) are compared with theory (blue solid line). In all panels the initial condition was $x_i(0) = x_i^*$.

In Fig. S2 we show the dependence of the mean and standard deviation of the QSD on α (when both quantities are normalized as in Fig. 4 in the main text), for gamma-distributed infection and recovery with an identical shape parameter. Naturally, this choice is arbitrary; however, while a lengthy analysis can be performed by doing many calculations in the phase space of (α_1, α_2) , we merely wanted to show that an analysis where all the reactions are non-Markovian is feasible. Notably, even a simplified choice of having an identical α value, highlights some of the interesting effects that emerge. As expected, when both processes vary together, the mean remains constant; yet, the standard deviation changes qualitatively in a manner similar to the recovery case (Fig. 4 in

the main text). This shows that, although the effects on the mean are exactly inverse for infection and recovery, their impact on fluctuations is not, as is evident from Eq. (12) in the main text.

POWER-LAW WAITING TIME DISTRIBUTION

In this section, we show that the asymptotic memory kernels can be obtained in a similar manner also for different WT distributions. Here we assume that infection is Markovian and recovery is non-Markovian, with a WT following a power-law distribution:

$$\psi_1(t) = \lambda_1 e^{-\lambda_1 t}, \quad \psi_2(t) = \frac{\lambda_2 \alpha}{(\alpha - 1) \left(1 + \frac{\lambda_2 t}{\alpha - 1}\right)^{\alpha+1}}, \quad (\text{S19})$$

with means of $\lambda_1 = NR_0 x_s x_i$ and $\lambda_2 = Nx_i$. Here, the shape parameter is bounded, $\alpha > 1$, to ensure a finite mean, and in the limit $\alpha \rightarrow \infty$ the distribution converges to an exponential one. Notably, the regime of $\alpha > 1$ in the gamma distribution does not exist here; namely, by choosing a power-law WT we can only increase the WT width and the corresponding memory strength.

Performing the explicit calculation of the normalized asymptotic memory kernel using section A, we find

$$\mathcal{M}_1 = R_0 x_i x_s, \quad \mathcal{M}_2 = \frac{\alpha x_i}{\alpha - 1} \frac{E_{\alpha+1}[(\alpha - 1)r_0 x_s]}{E_\alpha[(\alpha - 1)r_0 x_s]}, \quad (\text{S20})$$

where $E_m(z) \equiv \int_1^\infty e^{-z\tau} \tau^{-m} d\tau$ is the exponential integral function. At this point, one can plug these memory kernels into the late-time master equations and perform calculations along the same lines as in the main text, which allows to find the quantities of interest, e.g., outbreak-size distribution within the SIR model, or MTE within the SIS model.